Occupation Probabilities as Variables in Electronic Structure Theory: Cooper Pairing, OP-NSOFT-Cs,t, and the Homogeneous Electron Liquid

Ralph Gebauer[a], Morrel H. Cohen[b,c1], and Roberto Car[c,d1]

[a]The Abdus Salam International Centre for Theoretical Physics, 34151 Trieste, Italy; [b]Department of Physics and Astronomy, Rutgers University, Piscataway, NJ 08854; [c]Department of Chemistry, Princeton University, Princeton, NJ 08544; [d]Department of Physics, Princeton University, Princeton, NJ 08544

Abstract

The energy functional of a novel electronic structure theory, OP-NSOFT, has as variables the natural spin orbitals (NSO) of the trial function and their joint occupation probabilities in the search for the ground state energy. When occupancy is restricted to the spin-paired NSOs of DOCI, the resulting theory, OP-NSOFT-0, scales as M^3, with M the size of the one-electron basis set. Accurate results were obtained for small molecules, particularly near dissociation where single reference theories like DFT are inaccurate. The homogeneous electron liquid (HEL) could serve as a test bed of OP-NSOFT for condensed systems, but OP-NSOFT-0 reduces to the Hartree-Fock approximation for the HEL. Cooper pairing is introduced instead, both singlet pairing, OP-NOFT-Cs, and fully-polarized triplet pairing, OP-NSOFT-Ct. The former yields ⅓ of the diffusion-Monte-Carlo correlation energy, the latter ½ to ⅓ with decreasing electron density for r_s values between 1 and 10. Both yield the discontinuity in the single-particle occupation number required by the Luttinger theorem. Two-state joint occupation probabilities illustrate the importance of electron-electron small-angle scattering in establishing electron correlation in the unpolarized HEL.

1. Introduction

Much of the long search for useful *ab-initio* methods for computing the ground-state energies of atoms, molecules, and materials has been a struggle to balance accuracy against scalability. The computational costs of exact or near-exact methods such as Full Configuration Interaction (FCI) and its most accurate approximate forms increase combinatorially with the size M of the one-electron basis set. Theories which reduce that scaling must deal with several significant issues: the scaling itself; whether parameter-free forms can be found; the elimination of self-interaction, and the accuracy of the treatment of correlation. Hartree-Fock Theory (HF) scales asymptotically as M^3, is parameter- and self-interaction-free, but has no

[1] To whom correspondence may be addressed. Email: rcar@princeton.edu or mhcohen@prodigy.net.

correlation. Density-Functional Theory (DFT)[i,ii] scales asymptotically as M^3 but approximations to its functional have inaccuracies that grow as system fragments separate and there is difficulty with finding accurate, *parameter-free* versions that avoid self-interaction. Kohn-Sham DFT[ii] cannot capture the strong static correlation in dissociating fragments because it is a single reference theory. One-particle reduced density matrix functional theory (1RDMFT)[iii] can describe multi reference states. When the 1RDM is represented in terms of its eigenstates and eigenvalues, i.e. the natural orbitals (NO) and their occupation probabilities, the corresponding 1RDMFTs are called natural orbital functional theories (NOFTs). The primitive functionals of 1RDMFT that involve only two-index integrals scale as M^3. More accurate 1RDMFT functionals include 4-index integrals that increase the scaling to M^5[iv,v]. Most 1RDMFT functionals are parameter-free, cf. Pernal and Giesbertz[vi]. In 1RDMFT, there are natural orbital functionals (NOFs) that have the self-interaction problem[vii] but others that do not[viii,ix]. The latter theories have difficulty in accurately representing the one- and two-particle reduced density matrices (1RDM and 2RDM) simultaneously. Methods that specifically address that difficulty have been based on systematic refining of the necessary conditions for the 2RDM[x] and have achieved accuracy close to that of FCI[xi], but with computational cost scaling asymptotically at least as M^6.

We have recently introduced a class of occupation-probability-based, natural-spin-orbital functional theories, OP-NSOFT[xii]. In ref. xii, hereafter called **I**, it was specialized to time-reversal-invariant, singlet ground states with no local spin polarization. The theories start out from an FCI trial function Ψ expanded in Slater determinants (SD) $\Phi_{\boldsymbol{m}}$ in which the one-electron basis is the M natural spin orbitals (NSO) of the N-electron trial function,

$$\Psi = \sum_{\boldsymbol{m}} C_{\boldsymbol{m}} \Phi_{\boldsymbol{m}} , \quad (1)$$

with the $C_{\boldsymbol{m}}$ the expansion coefficients. Note that these differ from the exact NSOs introduced by Löwdin[xiii], which are derived from the ground state, and would converge to the NSOs of Löwdin in an exact theory. For the 1-electron basis functions actually to be the NSOs of the trial function, the expansion coefficients of the Slater determinants must satisfy an orthogonality constraint. The energy is then written as a linear functional of the one- and two-particle RDMs of Ψ. Using an explicit representation of the 2RDM eliminates self-interaction. The theory remains a variational 2RDM theory after imposition of the pair-difference condition and the sign approximations of **I**. The latter allows explicit expression of the energy functional in terms of the NSOs and their sole and joint occupation probabilities (OPs) of n NSOs, n-OPs with n=1…N and reinterpretation of that variational 2RDM theory as an OP-NSOFT. Parametric 2RDM methods have been introduced by Mazziotti[xiv] and Piris, et al.[xv], but neither uses the higher-order occupation probabilities we have introduced into the energy functional. Finally, the non-variational ξ-approximation of **I** replaces the N-OPs by 4-OPs. The OPs are taken as variables subject to bounds, sum rules, and the orthogonality constraint. The resulting theory scales asymptotically as M^5. More explicitly, three fundamental approximations have allowed

for this reduction from the combinatorial scaling of FCI: first, a variational[2] approximation to the orthogonality constraint, the pair difference constraint (PDC), that requires the SDs to differ by at least two NSOs; second, a variational approximation for the signs of the FCI expansion coefficients $C_{\boldsymbol{m}}$ of the SDs; and third, a non-variational reduction of the N-OPs in the exact correlation-energy functional to 4-OPs, the ξ-approximation. When the starting point is double-occupancy configuration interaction (DOCI) instead of FCI, all NSOs present in the SDs are spin paired, and consequently only 1- and 2-OPs enter the OP-NSOFT functional. The computations reported in **I** have shown that the resulting theory, OP-NSOFT-0, closely tracks DOCI along the dissociation curves of the various light molecules studied while scaling as M^3 instead of combinatorially. Close to but below DOCI for N > 4, it shares the latter's strengths and weaknesses for small molecules.

How accurate might OP-NSOFT be for extended systems, where scaling can become a major issue? Model extended systems for which the NSOs can be determined in advance are convenient for testing its accuracy. With known NSOs, the scaling of OP-NSOFT reduces from M^5 to M^4 and the scaling of OP-NSOFT-0 from M^3 to M^2, and the slow convergence of the NSOs characteristic of NSO-based theories is avoided. The homogeneous electron liquid (HEL) is a particularly interesting test model. Quantitatively accurate groundstate energy values are available for the HEL as a function of the Wigner–Seitz radius r_s from diffusion-Monte-Carlo (DMC) computations[xvi], providing the basis for a test of accuracy. The HEL has also been studied with 1RDMFT[xvii,3]. When applied to the HEL, OP-NSOFT-0 reduces to HF because homogeneity forces the matrix elements entering the correlation energy functional to vanish. Here we introduce instead forms of OP-NSOFT based on the singlet (OP-NSOFT-Cs, section 2) and polarized triplet (OP-NSOFT-Ct, section 3) Cooper pairings introduced in the BCS theory of superconductivity[xviii] and in the theory of the superfluidity of He-3[xix], respectively. In section 4, we report that we find a nonzero discontinuity in $p_1(k)$ at k_F and a nonzero correlation energy for the 3D HEL. Quantitative information on the 2-OPs obtained for the first time illuminates the processes that generate the electron correlation energy. We report a transition to the fully polarized state at $r_s \cong 7.5$ in section 5. Finally, in section 6 we assess what has been accomplished and discuss directions for further work.

2. The OP-NSOFT formalism

The OP-NSOFT energy functional derived in **I** by the imposition of the three scale-reducing approximations is, in the notation of **I**,

[2] A variational approximation imposes restrictions on the trial function.
[3] 1RDMFT is an OP-NSOFT in which the variables are the NSOs and the 1-OPs.

$$
\begin{aligned}
E[\psi, p_1, p_{11}, p_{111}, p_{1111}] &= \sum_i p_1\,(i)\hat{h}_{ii} \\
&+ \tfrac{1}{2}\sum_{i\neq j} p_{11}(ij)\big[\mathcal{J}_{ij} - \mathcal{K}_{ij}\big] \\
&+ \sum_{i<j\neq k<l} S(ij)\,S(kl)p^{1/2}_{1100}(ijkl)p^{1/2}_{0011}(ijkl)\xi(ijkl)[\mathcal{K}(ijkl) \\
&- \mathcal{K}(ijlk)] \qquad (2)
\end{aligned}
$$

$$
\xi(ijkl) = \frac{\sum_{m<n\neq ijkl} p^{1/2}_{1111}(ijmn)p^{1/2}_{1111}(klmn)}{\left[\sum_{m<n\neq ijkl} p_{1111}(ijmn)\sum_{m<n\neq ijkl} p_{1111}(klmn)\right]^{1/2}} \qquad (3)
$$

The indices $i, j \cdots = 1 \cdots M$ specify the NSOs $\psi_i, \psi_j \cdots$. The quantities $p_1, p_{11}, p_{1111}, p_{1100}\,, p_{0011}$ are occupation probabilities (OPs), the probabilities that the members of the set of NSOs specified by the indices serving as the arguments of those quantities are either simultaneously present in or absent from the SDs within the trial function. A subscript 1 indicates that the corresponding NSO is present; a subscript 0 indicates absence. An n-OP is the probability of occupation of n NSOs and has n subscripts and n arguments. The 2-OP $p_{11}(ij)$ is the probability that ψ_i and ψ_j are simultaneously present in the trial function, and the 4-OP $p_{1100}(ijkl)$ is the probability that ψ_i and ψ_j are present while ψ_k and ψ_l are absent. These 4-OPs of mixed occupancy are linear combinations of fully-occupied 4-, 3-, and 2-OPs,

$$
p_{1100}\,(ijkl) = p_{1111}(ijkl) - p_{111}(ijk) - p_{111}(ijl) + p_{11}(ij)\,, \quad (4a)
$$

$$
p_{0011}\,(ijkl) = p_{1111}(ijkl) - p_{111}(kli) - p_{111}(klj) + p_{11}(kl)\,. \quad (4b)
$$

The PDC forces all index pairs in the 4-OPs in (1) and (2), e.g. ij and kl, to have no common index. To derive Eqs. (4a,b) we introduce the idempotent variable $\nu_{i,\boldsymbol{m}}$, which specifies the occupation of ψ_i in $\Phi_{\boldsymbol{m}}$: $\nu_{i,\boldsymbol{m}} = 1$ if ψ_i is present in $\Phi_{\boldsymbol{m}}$ and $\nu_{i,\boldsymbol{m}} = 0$ if absent. Thus the fully occupied n-OP $p_{1\cdots1}(i_1 \cdots i_n)$ can be expressed as

$$
p_{1\cdots1}(i_1 \cdots i_n) = \sum_{\boldsymbol{m}} |C_{\boldsymbol{m}}|^2\, \nu_{i_1,\boldsymbol{m}} \cdots \nu_{i_n,\boldsymbol{m}}
$$

Similarly, the mixed occupancy 4-OPs $p_{1100}(ijkl)$ and $p_{0011}(ijkl)$ can be expressed as

$$
p_{1100}(ijkl) = \sum_{\boldsymbol{m}} |C_{\boldsymbol{m}}|^2\, \nu_{i,\boldsymbol{m}}\nu_{j,\boldsymbol{m}}\big(1-\nu_{k,\boldsymbol{m}}\big)\big(1-\nu_{l,\boldsymbol{m}}\big)\,,
$$

$$
p_{0011}(ijkl) = \sum_{\boldsymbol{m}} |C_{\boldsymbol{m}}|^2\, \big(1-\nu_{i,\boldsymbol{m}}\big)\big(1-\nu_{j,\boldsymbol{m}}\big)\nu_{k,\boldsymbol{m}}\nu_{l,\boldsymbol{m}}\,.
$$

Expanding the parentheses in this definition of the mixed 4-OPs and using this definition of the pure n-OPs yields (4a,b).

The NSOs enter the functional (2) implicitly through their presence in the various matrix elements. The first term on the rhs of (2) is the single-particle energy functional. In it, $\hat{h}$ is the single-particle Hamiltonian, and $h_{ii} = \big(\psi_i, \hat{h}\psi_i\big)$ is its diagonal matrix element. The second term

on the rhs is the sum of the Hartree and exchange energy functionals. $\mathcal{J}_{ij} = \left(\psi_i\psi_j, \hat{w}\psi_i\psi_j\right)$ and $\mathcal{K}_{ij} = \left(\psi_i\psi_j, \hat{w}\psi_j\psi_i\right)$ are the Coulomb and exchange integrals, respectively, with $\hat{w}$ the Coulomb interaction. The third term is the correlation energy functional. In it, $\mathcal{K}_{ijkl}$ $=\left(\psi_i\psi_j, \hat{w}\psi_k\psi_l\right)$ is the direct matrix element of $\hat{w}$ that scatters a pair of electrons from the states kl to the states ij, and $\mathcal{K}_{ijlk} = \left(\psi_i\psi_j, \hat{w}\psi_l\psi_k\right)$ is the corresponding exchange matrix element.

The signs of the SD coefficients are reduced to $S(ij)$ and $S(kl)$ in (2) by the variational sign approximation. They are set prior to the search for the infimum of the functional. The rule for setting the signs stated in Section S1 of the supplementary information to **I** holds when the matrix element $\mathcal{K}(ijkl) - \mathcal{K}(ijlk)$ is positive, as will be the case for the HEL once the above pairing approximations referred to in the introduction are imposed. The sign rule was obtained by setting the coefficient signs to their values in the lowest order of an NSO version of Brillouin-Wigner perturbation theory, a variational approximation that may not be accurate for systems more complex than the HEL and the small molecules of **I**. Nevertheless, we have established that for some systems the phase dilemma that stems from the necessity of carrying out minimization over the large number of possible combinations of coefficient signs[xx] can be avoided.

$\xi(ijkl)$, (3), is the ξ-approximation. It is a nonvariational replacement of the exact N-OPs that enter the FCI correlation energy functional by 4-OPs like the $p_{1111}(ijmn)$ in (3). As discussed in **I**, ξ has the same bounds,

$$0 \leq \xi(ijkl) \leq 1, \quad (5)$$

as the exact quantity it approximates. The OP-NSOFT approximation to the ground-state is obtained by searching for the infimal value of the energy functional (2) in the space of the variables $\psi, p_1, p_{11}, p_{111}, p_{1111}$ subject to a set of necessary conditions.[xxi]

3. Cooper pairing for the HEL: Singlet pairing in OP-NSOFT-Cs

3.1 The OP-NSOFT-Cs functional, spins explicit

The HEL NSOs are plane waves $\phi_{\boldsymbol{k}}(\boldsymbol{r})$ with wave number $\boldsymbol{k}$ times spinors $\chi_s(\sigma)$ with spin–state s so that the index i becomes $\boldsymbol{k}s$. Just as OP-NSOFT-0 evolved from DOCI, OP-NSOFT-Cs evolves from a different restricted version of CI, CsCI, in which when the NSO $\boldsymbol{k}\uparrow$ is present in an SD, so is the NSO $-\boldsymbol{k}\downarrow$. Each SD is formed of time-reversed pairs, singlet Cooper pairs. Note that the N-projected BCS wave function is a specific CsCI wave function for which all n-OPs are products of n 1-OPs. The N-electron CsCI functions are not N-projections of the BCS wave function in general, and their n-OPs are not restricted to products of 1-OPs. The resulting OP-NSOFT, OP-NSOFT-Cs is thus more general and more accurate than earlier attempts to use the BCS wave function to approximate the 2RDM for molecular systems[xxii] and for extended systems.[xxiii] These approximations based on the BCS wave function were abandoned because

they overcorrelate, especially at dissociation where fixed particle number is essential. The N-projected BCS wave function eliminates that difficulty and has been used to create the so called Antisymmetrized Products of identical Geminals (APG) formalism.[xxiv] As implied above, pairs are uncorrelated in APG, and it is consequently less accurate than OP-NSOFT-Cs.

CsCI clearly satisfies the PDC. The PDC and the Cooper pairing require that the index pairs ij and kl in the correlation energy functional become $\boldsymbol{k}\uparrow,-\boldsymbol{k}\downarrow$ and $\boldsymbol{k}'\uparrow,-\boldsymbol{k}'\downarrow$, respectively. The self-interaction of the uniform background, the Hartree term, and the electron-uniform background interaction all cancel, leaving only the kinetic energy $\epsilon(k)$ in the single-particle functional and only the exchange energy in the Hartree/exchange functional. The energy functional (2), (3) becomes

$$E[p_1,p_{11},p_{111},p_{1111}] = \sum_{\boldsymbol{ks}} p_1(\boldsymbol{ks})\epsilon(k) - \tfrac{1}{2}\sum_{\boldsymbol{k}\neq\boldsymbol{k}',s} p_{11}(\boldsymbol{ks}\boldsymbol{k}'s)w(|\boldsymbol{k}-\boldsymbol{k}'|) + \sum_{\boldsymbol{k}\neq\boldsymbol{k}'} S(\boldsymbol{k}\uparrow,-\boldsymbol{k}\downarrow)\,S(\boldsymbol{k}'\uparrow,-\boldsymbol{k}'\downarrow)p^{1/2}_{1100}(\boldsymbol{k}\uparrow,-\boldsymbol{k}\downarrow;\boldsymbol{k}'\uparrow,-\boldsymbol{k}'\downarrow)p^{1/2}_{0011}(\boldsymbol{k}\uparrow,-\boldsymbol{k}\downarrow;\boldsymbol{k}'\uparrow,-\boldsymbol{k}'\downarrow)\xi(\boldsymbol{k}\uparrow,-\boldsymbol{k}\downarrow;\boldsymbol{k}'\uparrow,-\boldsymbol{k}'\downarrow)w(|\boldsymbol{k}-\boldsymbol{k}'|)\,, \quad (6)$$

$$\xi(\boldsymbol{k}\uparrow,-\boldsymbol{k}\downarrow;\boldsymbol{k}'\uparrow,-\boldsymbol{k}'\downarrow) = \frac{\sum_{\boldsymbol{l}\neq\boldsymbol{k}\boldsymbol{k}'} p^{1/2}_{1111}(\boldsymbol{k}\uparrow,-\boldsymbol{k}\downarrow;\boldsymbol{l}\uparrow,-\boldsymbol{l}\downarrow)p^{1/2}_{1111}(\boldsymbol{k}'\uparrow,-\boldsymbol{k}'\downarrow;\boldsymbol{l}\uparrow,-\boldsymbol{l}\downarrow)}{[\sum_{\boldsymbol{l}\neq\boldsymbol{k}\boldsymbol{k}'} p_{1111}(\boldsymbol{k}\uparrow,-\boldsymbol{k}\downarrow;\boldsymbol{l}\uparrow,-\boldsymbol{l}\downarrow)\sum_{\boldsymbol{l}\neq\boldsymbol{k}\boldsymbol{k}'} p_{1111}(\boldsymbol{k}'\uparrow,-\boldsymbol{k}'\downarrow;\boldsymbol{l}\uparrow,-\boldsymbol{l}\downarrow)]^{1/2}}\,. \quad (7)$$

The interaction matrix element in (6),

$$w(|\boldsymbol{q}|) = \frac{4\pi e^2}{\Omega q^2}\,, \quad (8)$$

is the Fourier transform of the Coulomb interaction with Ω the quantization volume. Because it is positive, the sign rules are the same as in OP-NSOFT-0 and are given in section S1 of **I**,

$$S(\boldsymbol{k}\uparrow,-\boldsymbol{k}\downarrow) = +1, k \leq k_F;\ S(\boldsymbol{k}\uparrow,-\boldsymbol{k}\downarrow) = -1, k > k_F\,. \quad (9)$$

3.2 The OP-NSOFT-Cs functional: from 4-OPs to 2-OPs

The formal definition of $p_1(\boldsymbol{ks})$ is

$$p_1(\boldsymbol{ks}) = \sum_{\boldsymbol{m}} |C_{\boldsymbol{m}}|^2\, \nu_{\boldsymbol{ks},\boldsymbol{m}}\,, \quad (10)$$

where the occupation designator $\nu_{\boldsymbol{ks},\boldsymbol{m}}$ has the values

$$\nu_{\boldsymbol{ks},\boldsymbol{m}} = 1, \boldsymbol{ks} \in \boldsymbol{m}; = 0, \boldsymbol{ks} \notin \boldsymbol{m}\,. \quad (11)$$

Because each SD is comprised of N occupied NSOs, there is a sum rule obeyed by the $\nu_{\boldsymbol{ks},\boldsymbol{m}}$,

$$\sum_{\boldsymbol{ks}} \nu_{\boldsymbol{ks},\boldsymbol{m}} = N, \forall \boldsymbol{m}\,. \quad (12)$$

The time-reversed pairing requires that

$$\nu_{\boldsymbol{k}\uparrow,\boldsymbol{m}} = \nu_{-\boldsymbol{k}\downarrow,\boldsymbol{m}}\,, \forall \boldsymbol{m}\,, \quad (13)$$

and inversion symmetry requires that

$$\nu_{-\boldsymbol{k}\downarrow,\boldsymbol{m}} = \nu_{\boldsymbol{k}\downarrow,\boldsymbol{m}}\,, \quad (14)$$

so that the 1-OP is spin independent

$$p_1(\boldsymbol{k}\uparrow) = p_1(\boldsymbol{k}\downarrow) = p_1(\boldsymbol{k})\,. \quad (15)$$

The formal definition of $p_{11}(\boldsymbol{k}s\boldsymbol{k}'s)$ is

$$p_{11}(\boldsymbol{k}s\boldsymbol{k}'s) = \sum_{\boldsymbol{m}} |C_{\boldsymbol{m}}|^2\, \nu_{\boldsymbol{k}s,\boldsymbol{m}}\nu_{\boldsymbol{k}'s,\boldsymbol{m}}\,. \quad (16)$$

It is spin independent according to (13) and (14),

$$p_{11}(\boldsymbol{k}\uparrow\boldsymbol{k}'\uparrow) = p_{11}(\boldsymbol{k}\downarrow\boldsymbol{k}'\downarrow) = p_{11}(\boldsymbol{k}\boldsymbol{k}')\,. \quad (17)$$

The formal definitions of the mixed 4-OPs in (6) are

$$p_{1100}(\boldsymbol{k}\uparrow,-\boldsymbol{k}\downarrow;\boldsymbol{k}'\uparrow,-\boldsymbol{k}'\downarrow) = \sum_{\boldsymbol{m}} |C_{\boldsymbol{m}}|^2\, \nu_{\boldsymbol{k}\uparrow,\boldsymbol{m}}\nu_{-\boldsymbol{k}\downarrow,\boldsymbol{m}}\big(1-\nu_{\boldsymbol{k}'\uparrow,\boldsymbol{m}}\big)\big(1-\nu_{-\boldsymbol{k}'\downarrow,\boldsymbol{m}}\big)\,, \quad (18a)$$

$$p_{0011}(\boldsymbol{k}\uparrow,-\boldsymbol{k}\downarrow;\boldsymbol{k}'\uparrow,-\boldsymbol{k}'\downarrow) = \sum_{\boldsymbol{m}} |C_{\boldsymbol{m}}|^2\, \big(1-\nu_{\boldsymbol{k}\uparrow,\boldsymbol{m}}\big)\big(1-\nu_{-\boldsymbol{k}\downarrow,\boldsymbol{m}}\big)\nu_{\boldsymbol{k}'\uparrow,\boldsymbol{m}}\nu_{-\boldsymbol{k}'\downarrow,\boldsymbol{m}}\,. \quad (18b)$$

As (11) implies that the $\nu_{\boldsymbol{k}\uparrow,\boldsymbol{m}}$ are idempotent, imposing the pairing condition (13) reduces the 4-OPs of (18a,b) to 2-OPs

$$p_{1100}(\boldsymbol{k}\uparrow,-\boldsymbol{k}\downarrow;\boldsymbol{k}'\uparrow,-\boldsymbol{k}'\downarrow) = \sum_{\boldsymbol{m}} |C_{\boldsymbol{m}}|^2\, \nu_{\boldsymbol{k}\uparrow,\boldsymbol{m}}\big(1-\nu_{\boldsymbol{k}'\uparrow,\boldsymbol{m}}\big) = p_{10}(\boldsymbol{k}\uparrow\boldsymbol{k}'\uparrow)\,, \quad (19a)$$

$$p_{0011}(\boldsymbol{k}\uparrow,-\boldsymbol{k}\downarrow;\boldsymbol{k}'\uparrow,-\boldsymbol{k}'\downarrow) = \sum_{\boldsymbol{m}} |C_{\boldsymbol{m}}|^2\, \big(1-\nu_{\boldsymbol{k}\uparrow,\boldsymbol{m}}\big)\nu_{\boldsymbol{k}'\uparrow,\boldsymbol{m}} = p_{01}(\boldsymbol{k}\uparrow\boldsymbol{k}'\uparrow). \quad (19b)$$

Expanding the parentheses in (19a,b) simplifies (4a,b) to

$$p_{10}(\boldsymbol{k}\uparrow\boldsymbol{k}'\uparrow) = p_{10}(\boldsymbol{k}\boldsymbol{k}') = p_1(\boldsymbol{k}) - p_{11}(\boldsymbol{k}\boldsymbol{k}')\,, \quad (20a)$$

$$p_{01}(\boldsymbol{k}\uparrow\boldsymbol{k}'\uparrow) = p_{01}(\boldsymbol{k}\boldsymbol{k}') = p_1(\boldsymbol{k}') - p_{11}(\boldsymbol{k}\boldsymbol{k}')\,, \quad (20b)$$

(13) reduces the order of ξ as well; (7) becomes

$$\xi(\boldsymbol{k}\boldsymbol{k}') = \frac{\sum_{\boldsymbol{l}\neq\boldsymbol{k}\boldsymbol{k}'} p_{11}^{1/2}(\boldsymbol{k}\boldsymbol{l})p_{11}^{1/2}(\boldsymbol{k}'\boldsymbol{l})}{[\sum_{\boldsymbol{l}\neq\boldsymbol{k}\boldsymbol{k}'} p_{11}(\boldsymbol{k}\boldsymbol{l})\sum_{\boldsymbol{l}\neq\boldsymbol{k}\boldsymbol{k}'} p_{11}(\boldsymbol{k}'\boldsymbol{l})]^{1/2}}\,. \quad (21)$$

Similarly, the signs in (6) and (9) depend only on the single variable $\boldsymbol{k}$,

$$S(\boldsymbol{k}\uparrow,-\boldsymbol{k}\downarrow) = S(\boldsymbol{k}) = +1, k \le k_F;\ = -1, k > k_F\,. \quad (22)$$

The functional becomes

$$\begin{aligned} E[p_1,p_{11}] = 2\sum_{\boldsymbol{k}} & p_1(\boldsymbol{k})\epsilon(k) \\ & - \sum_{\boldsymbol{k}\neq\boldsymbol{k}'} p_{11}(\boldsymbol{k}\boldsymbol{k}')w(|\boldsymbol{k}-\boldsymbol{k}'|) \\ & + \sum_{\boldsymbol{k}\neq\boldsymbol{k}'} S(\boldsymbol{k})\,S(\boldsymbol{k}')p_{10}^{1/2}(\boldsymbol{k}\boldsymbol{k}')p_{01}^{1/2}(\boldsymbol{k}\boldsymbol{k}')\xi(\boldsymbol{k}\boldsymbol{k}')w(|\boldsymbol{k}-\boldsymbol{k}'|)\,, \end{aligned} \quad (23)$$

and is supplemented by (20a,b), (21), and (22).

The discontinuity in the signs imposed by (22) at the initiation of the search for the infimum of $E[p_1, p_{11}]$ guarantees the existence of a discontinuity in $p_1(\boldsymbol{k})$ at k_F in accordance with the Luttinger theorem.[xxv]

3.3 Bounds and sum rules imposed on p_1 and p_{11}

The quantities $p_1(\boldsymbol{k})$ and $p_{11}(\boldsymbol{k}\boldsymbol{k}')$ are subject to constraints, sum rules and bounds, as they vary during the search for the infimum value of $E[p_1, p_{11}]$. As a probability, $p_1(\boldsymbol{k})$ must have the bounds

$$0 \leq p_1(\boldsymbol{k}) \leq 1 \quad (24)$$

evident from (10). The 1-OP sum rule is

$$\sum_{\boldsymbol{k}} p_1(\boldsymbol{k}) = ½ \sum_{\boldsymbol{k}s} p_1(\boldsymbol{k}s) = ½N\,. \quad (25)$$

The sum rule on $p_{11}(\boldsymbol{k}, \boldsymbol{k}')$ follows from that on $p_{11}(\boldsymbol{k}s\boldsymbol{k}'s')$,

$$\sum_{\boldsymbol{k}'s' \neq \boldsymbol{k}s} p_{11}(\boldsymbol{k}s\boldsymbol{k}'s') = \sum_{\boldsymbol{m}} |C_{\boldsymbol{m}}|^2\, \nu_{\boldsymbol{k}s,\boldsymbol{m}} \sum_{\boldsymbol{k}'s' \neq \boldsymbol{k}s} \nu_{\boldsymbol{k}'s',\boldsymbol{m}} = (N-1)p_1(\boldsymbol{k}s)\,, \quad (26)$$

that is,

$$2 \sum_{\boldsymbol{k}' \neq \boldsymbol{k}} p_{11}(\boldsymbol{k}\boldsymbol{k}') = (N-2)p_1(\boldsymbol{k})\,. \quad (27)$$

(27) can be used to simplify the sums in the denominator of $\xi(\boldsymbol{k}\boldsymbol{k}')$ in (21),

$$\sum_{\boldsymbol{l} \neq \boldsymbol{k}\boldsymbol{k}'} p_{11}(\boldsymbol{k}\boldsymbol{l}) = ½(N-2)p_1(\boldsymbol{k}) - p_{11}(\boldsymbol{k}\boldsymbol{k}'), \quad (28a)$$

$$\sum_{\boldsymbol{l} \neq \boldsymbol{k}\boldsymbol{k}'} p_{11}(\boldsymbol{k}'\boldsymbol{l}) = ½(N-2)p_1(\boldsymbol{k}') - p_{11}(\boldsymbol{k}\boldsymbol{k}'). \quad (28b)$$

The derivation of the bounds on $p_{11}(\boldsymbol{k}\boldsymbol{k}')$ is more complex and will not be given here. We refer instead to **I** and references therein. Those bounds are

$$sup\{p_1(\boldsymbol{k}) + p_1(\boldsymbol{k}') - 1{,}0\} \leq p_{11}(\boldsymbol{k}\boldsymbol{k}') \leq inf\{p_1(\boldsymbol{k}), p_1(\boldsymbol{k}')\}\,, \quad (29)$$

$$sup\{p_1(\boldsymbol{k}) + p_1(\boldsymbol{k}') + p_1(\boldsymbol{k}'') - 1{,}0\} \leq p_{11}(\boldsymbol{k}\boldsymbol{k}') + p_{11}(\boldsymbol{k}'\boldsymbol{k}'') + p_{11}(\boldsymbol{k}\boldsymbol{k}'')\,. \quad (30)$$

Eq. (29) is a (2,2) condition and (30) a (2,3) condition.[xxi]

3.4 Large N

In the thermodynamic limit,

$$\frac{E}{N} \to \mathcal{E}; E, N \to \infty\,, \quad (31a)$$

$$\frac{N}{\Omega} \to n; N, \Omega \to \infty\,, \quad (31b)$$

the sums can be transformed to integrals

$$\sum_{\boldsymbol{k}} (\cdot) \to \frac{\Omega}{(2\pi)^3} \int d^3\boldsymbol{k}\, (\cdot)\,. \quad (32)$$

It is convenient to scale the wave vector to the Fermi wave number

$$\bar{\boldsymbol{k}} = \frac{\boldsymbol{k}}{k_F} \ . \quad (33)$$

The energy functional becomes

$$\mathcal{E}[p_1, p_{11}] = \frac{3}{4\pi}\int d^3\bar{\boldsymbol{k}}\, p_1(\bar{\boldsymbol{k}})\frac{\bar{k}^2}{2}{k_F}^2 - \frac{9n}{16\pi}\iint d^3\bar{\boldsymbol{k}}d^3\bar{\boldsymbol{k}}' p_{11}(\bar{\boldsymbol{k}}\bar{\boldsymbol{k}}')\frac{1}{{k_F}^2\left|\bar{\boldsymbol{k}} - \bar{\boldsymbol{k}}'\right|^2}$$
$$+ \frac{9n}{16\pi}\iint d^3\bar{\boldsymbol{k}}d^3\bar{\boldsymbol{k}}' S(\bar{k})S(\bar{k}')p_{10}^{½}(\bar{\boldsymbol{k}}\bar{\boldsymbol{k}}')p_{01}^{½}(\bar{\boldsymbol{k}}\bar{\boldsymbol{k}}')\xi(\bar{\boldsymbol{k}}\bar{\boldsymbol{k}}')\frac{1}{{k_F}^2\left|\bar{\boldsymbol{k}} - \bar{\boldsymbol{k}}'\right|^2} \quad (34)$$

$$\xi(\bar{\boldsymbol{k}}\bar{\boldsymbol{k}}') = \frac{\int d^3\bar{\boldsymbol{l}}\, p_{11}^{½}(\bar{\boldsymbol{k}}\bar{\boldsymbol{l}})p_{11}^{½}(\bar{\boldsymbol{k}}'\bar{\boldsymbol{l}})}{\left[\int d^3\bar{\boldsymbol{l}}\, p_{11}(\bar{\boldsymbol{k}}\bar{\boldsymbol{l}})\int d^3\bar{\boldsymbol{l}}\, p_{11}(\bar{\boldsymbol{k}}'\bar{\boldsymbol{l}})\right]^{½}} \quad (35)$$

The sum rules become

$$\frac{3}{4\pi}\int d^3\bar{\boldsymbol{k}}\, p_1(\bar{\boldsymbol{k}}) = 1\,, \quad (36)$$

$$\frac{3}{4\pi}\int d^3\bar{\boldsymbol{k}}'\, p_{11}(\bar{\boldsymbol{k}}\bar{\boldsymbol{k}}') = p_1(\bar{\boldsymbol{k}})\,. \quad (37)$$

3.5 Isotropy

The isotropy of the HEL implies that quantities that depend on a single wave vector $\bar{\boldsymbol{k}}$ are functions only of its magnitude $\bar{k}$ and that functions that depend on two wave vectors $\bar{\boldsymbol{k}}, \bar{\boldsymbol{k}}'$ are functions only of their magnitudes $\bar{k}, \bar{k}'$ and the cosine $\mu_{\bar{\boldsymbol{k}}\bar{\boldsymbol{k}}'}$ of the angle $\theta_{\bar{\boldsymbol{k}}\bar{\boldsymbol{k}}'}$ between them. The energy functional simplifies to

$$\mathcal{E}[p_1, p_{11}]$$
$$= \frac{3}{2}{k_F}^2\int_0^\infty d\bar{k}p_1(\bar{k})\bar{k}^4 - \frac{9\pi n}{2{k_F}^2}\iint_0^\infty d\bar{k}d\bar{k}'\int_{-1}^{1} d\mu_{\bar{\boldsymbol{k}}\bar{\boldsymbol{k}}'}p_{11}(\bar{k}\bar{k}'\mu_{\bar{\boldsymbol{k}}\bar{\boldsymbol{k}}'})\frac{\bar{k}^2\bar{k}'^2}{\bar{k}^2 + \bar{k}'^2 - 2\bar{k}\bar{k}'\mu_{\bar{\boldsymbol{k}}\bar{\boldsymbol{k}}'}}$$
$$+ \frac{9\pi n}{2{k_F}^2}\iint_0^\infty d\bar{k}d\bar{k}' S(\bar{k})S(\bar{k}')p_{10}^{½}(\bar{k}\bar{k}'\mu_{\bar{\boldsymbol{k}}\bar{\boldsymbol{k}}'})p_{01}^{½}(\bar{k}\bar{k}'\mu_{\bar{\boldsymbol{k}}\bar{\boldsymbol{k}}'})\xi(\bar{k}\bar{k}'\mu_{\bar{\boldsymbol{k}}\bar{\boldsymbol{k}}'})\frac{\bar{k}^2\bar{k}'^2}{\bar{k}^2 + \bar{k}'^2 - 2\bar{k}\bar{k}'\mu_{\bar{\boldsymbol{k}}\bar{\boldsymbol{k}}'}},$$
$$(38)$$

$$p_{10}(\bar{k}\bar{k}'\mu_{\bar{\boldsymbol{k}}\bar{\boldsymbol{k}}'}) = p_1(\bar{\boldsymbol{k}}) - p_{11}(\bar{k}\bar{k}'\mu_{\bar{\boldsymbol{k}}\bar{\boldsymbol{k}}'})\,, \quad (39a)$$

$$p_{01}(\bar{k}\bar{k}'\mu_{\bar{\boldsymbol{k}}\bar{\boldsymbol{k}}'}) = p_1(\bar{\boldsymbol{k}}') - p_{11}(\bar{k}\bar{k}'\mu_{\bar{\boldsymbol{k}}\bar{\boldsymbol{k}}'})\,. \quad (39b)$$

$\xi(\bar{\boldsymbol{k}}\bar{\boldsymbol{k}}')$, (35), is more complex as it involves 3 vectors, $\bar{\boldsymbol{k}}$, $\bar{\boldsymbol{k}}'$, and $\bar{\boldsymbol{l}}$. We take $\bar{\boldsymbol{k}}$ as the polar axis and measure the azimuthal angle $\phi_{\boldsymbol{l}}$ of $\bar{\boldsymbol{l}}$ from the $\bar{\boldsymbol{k}}$, $\bar{\boldsymbol{k}}'$-plane so that

$$\mu_{\boldsymbol{k}'\boldsymbol{l}} = cos\theta_{\boldsymbol{k}'\boldsymbol{l}} = \mu_{\boldsymbol{k}\boldsymbol{k}'}\mu_{\boldsymbol{k}\boldsymbol{l}} + sin\theta_{\boldsymbol{k}\boldsymbol{k}'}sin\theta_{\boldsymbol{k}\boldsymbol{l}}cos\phi_{\boldsymbol{l}}\,. \quad (40)$$

Insert the sum rule (37) into the denominator of (35) to obtain

$$\xi(\bar{k}\bar{k}'\mu_{\bar{\boldsymbol{k}}\bar{\boldsymbol{k}}'}) = \frac{3\int_0^\infty d\bar{l}\,\bar{l}^2\int_{-1}^{1} d\mu_{\bar{\boldsymbol{k}}\bar{\boldsymbol{l}}}\int_0^{2\pi} d\varphi_{\bar{l}}\, p_{11}^{½}(\bar{k}\bar{l}\mu_{\bar{\boldsymbol{k}}\bar{\boldsymbol{l}}})p_{11}^{½}(\bar{k}'\bar{l}\mu_{\bar{\boldsymbol{k}}'\bar{\boldsymbol{l}}})}{2p_1(\bar{k})^{½}p_1(\bar{k}')^{½}} \quad (41)$$

with (40) understood.
The sum rules become

$$\int_0^\infty d\,\bar{k} p_1(\bar{k})\bar{k}^2 = ⅓\,, \quad (42)$$

$$\int_0^\infty d\,\bar{k}' \int_{-1}^{1} d\,\mu_{\overline{\boldsymbol{k}\boldsymbol{k}'}} p_{11}(\bar{k}\bar{k}'\mu_{\overline{\boldsymbol{k}\boldsymbol{k}'}})\bar{k}'^2 = ⅔\,. \quad (43)$$

The bounds become

$$0 \le p_1(k) \le 1\,, \quad (44)$$

$$sup\{p_1(k) + p_1(k') - 1{,}0\} \le p_{11}(kk'\mu_{\boldsymbol{k}\boldsymbol{k}'}) \le inf\{p_1(k), p_1(k')\}\,, \quad (45)$$

$$sup\{p_1(k) + p_1(k') + p_1(k'') - 1{,}0\} \le p_{11}(kk'\mu_{\boldsymbol{k}\boldsymbol{k}'}) + p_{11}(k'k''\mu_{\boldsymbol{k}'\boldsymbol{k}''}) + p_{11}(kk''\mu_{\boldsymbol{k}\boldsymbol{k}''})\,. \quad (46)$$

Equations (38)-(46) are the working formulae of OP-NSOFT-Cs for the HEL.

4. Cooper pairing for the HEL: Fully polarized triplet pairing; OP-NSOFT-Ct

In the fully polarized HEL only the NSOs $\boldsymbol{k}\uparrow$ are occupied. In the triplet-pairing approximation of OP-NSOFT-Ct, only the paired NSOs $\boldsymbol{k}\uparrow$ and $-\boldsymbol{k}\uparrow$ appear in the SDs. Having given the development of OP-NSOFT-Cs in detail, there is no need for such detail for OP-NSOFT-Ct, for which the energy functional is

$$E[p_1, p_{11}] = \sum_{\boldsymbol{k}} p_1(\boldsymbol{k})\epsilon(k) - ½ \sum_{\boldsymbol{k}\neq\boldsymbol{k}'} p_{11}(\boldsymbol{k}\boldsymbol{k}')w(|\boldsymbol{k}-\boldsymbol{k}'|) + \sum_{\boldsymbol{k}\neq\boldsymbol{k}'(half\ space)} S(\boldsymbol{k})\,S(\boldsymbol{k}')p_{10}^{½}(\boldsymbol{k},\boldsymbol{k}')p_{01}^{½}(\boldsymbol{k},\boldsymbol{k}')\xi(\boldsymbol{k},\boldsymbol{k}')[w(|\boldsymbol{k}-\boldsymbol{k}'|) - w(|\boldsymbol{k}+\boldsymbol{k}'|)]\,, \quad (47)$$

$$\xi(\boldsymbol{k},\boldsymbol{k}') = \frac{\sum_{\boldsymbol{l}\neq\boldsymbol{k}\boldsymbol{k}'(\boldsymbol{half\ space})} p_{11}^{½}(\boldsymbol{k},\boldsymbol{l})p_{11}^{½}(\boldsymbol{k}',\boldsymbol{l})}{\left[\sum_{\boldsymbol{l}\neq\boldsymbol{k}\boldsymbol{k}'(\boldsymbol{half\ space})} p_{11}(\boldsymbol{k},\boldsymbol{l}) \sum_{\boldsymbol{l}\neq\boldsymbol{k}\boldsymbol{k}'(\boldsymbol{half\ space})} p_{11}(\boldsymbol{k}',\boldsymbol{l})\right]^{½}}\,. \quad (48)$$

As before, in the cases of spin and singlet Cooper pairing, the 4-OPs reduce to 2-OPs. In the correlation energy functional, the pair ij becomes $\boldsymbol{k}\uparrow, -\boldsymbol{k}\uparrow$, and the sum on $\boldsymbol{k}$ is only over the half space as the pair $\boldsymbol{k}\uparrow, -\boldsymbol{k}\uparrow$ is identical to the pair $-\boldsymbol{k}\uparrow, \boldsymbol{k}\uparrow$. The spin index has been dropped as all spins are up. The sign rules are the same as for spin and singlet Cooper pairing, Eq. (9).

The reduction of the wave-vector dependences of the OPs imposed by isotropy is similar to that for singlet pairing, cf. Eqs. (38)-(46), with the following exceptions: Recall that $p_{11}(\boldsymbol{k}\boldsymbol{k}')$ is

$$p_{11}(\boldsymbol{k}\boldsymbol{k}') = \sum_{\boldsymbol{m}} |C_{\boldsymbol{m}}|^2 \, \nu_{\boldsymbol{k},\boldsymbol{m}} \nu_{\boldsymbol{k}',\boldsymbol{m}} \quad (49)$$

and that

$$\nu_{\boldsymbol{k}',\boldsymbol{m}} = \nu_{-\boldsymbol{k}',\boldsymbol{m}} \quad (50)$$

because of the triplet Cooper pairing. Together they imply that

$$p_{11}(\boldsymbol{k}\boldsymbol{k}') = p_{11}(\boldsymbol{k}, -\boldsymbol{k}') \,, \quad (51)$$

i. e. that

$$p_{11}(kk'\mu_{\boldsymbol{k}\boldsymbol{k}'}) = p_{11}(kk', -\mu_{\boldsymbol{k}\boldsymbol{k}'}) \,, \quad (52)$$

an even function of $\mu_{\boldsymbol{k}\boldsymbol{k}'}$. $p_{10}(\boldsymbol{k}\boldsymbol{k}')$ and $p_{01}(\boldsymbol{k}\boldsymbol{k}')$ enter (47) in sums over the half spaces of $\boldsymbol{k}$ and $\boldsymbol{k}'$, but we shall extend the sums to the full spaces. (20a,b) also hold for triplet pairing, and, with (51) and (52), imply that $p_{10}(kk'\mu_{\boldsymbol{k}\boldsymbol{k}'})$ and $p_{01}(kk'\mu_{\boldsymbol{k}\boldsymbol{k}'})$ are even functions of $\mu_{\boldsymbol{k}\boldsymbol{k}'}$. The same holds for $\xi(\boldsymbol{k}, \boldsymbol{k}') = \xi(k, k', \mu_{\boldsymbol{k}\boldsymbol{k}'})$. On the other hand, the matrix element $[w(|\boldsymbol{k}-\boldsymbol{k}'|) - w(|\boldsymbol{k}+\boldsymbol{k}'|)]$ is positive in the positive half spaces, i.e. for positive $\mu_{\boldsymbol{k}\boldsymbol{k}'}$, but it is an odd function of $\boldsymbol{k}'$ and therefore of $\mu_{\boldsymbol{k}\boldsymbol{k}'}$ in the full $\boldsymbol{k}'$ space. To extend the sums to the full spaces, it is necessary to make the matrix element an even function of $\boldsymbol{k}'$ by taking its magnitude. The result is

$$\begin{aligned} E[p_1, p_{11}] = \sum_{\boldsymbol{k}} p_1(k)\epsilon(k) \\ - \tfrac{1}{2} \sum_{\boldsymbol{k}\neq\boldsymbol{k}'} p_{11}(kk'\mu_{\boldsymbol{k}\boldsymbol{k}'}) w(|\boldsymbol{k}-\boldsymbol{k}'|) \\ + \tfrac{1}{4} \sum_{\boldsymbol{k}\neq\boldsymbol{k}'} S(k)\, S(k') p_{10}^{1/2}(kk'\mu_{k'}) p_{01}^{1/2}(kk'\mu_{\boldsymbol{k}\boldsymbol{k}'}) \xi(kk'\mu_{\boldsymbol{k}\boldsymbol{k}'}) |w(|\boldsymbol{k}-\boldsymbol{k}'|) \\ - w(|\boldsymbol{k}+\boldsymbol{k}'|)| \end{aligned} \quad (53)$$

$$\xi(\boldsymbol{k}, \boldsymbol{k}') = \frac{\sum_{\boldsymbol{l}\neq\boldsymbol{k}\boldsymbol{k}'} p_{11}^{1/2}(kl\mu_{\boldsymbol{k}\boldsymbol{l}}) p_{11}^{1/2}(k'l\mu_{\boldsymbol{k}'\boldsymbol{l}})}{[\sum_{\boldsymbol{l}\neq\boldsymbol{k}\boldsymbol{k}'} p_{11}(kl\mu_{\boldsymbol{k}\boldsymbol{l}}) \sum_{\boldsymbol{l}\neq\boldsymbol{k}\boldsymbol{k}'} p_{11}(k'l\mu_{\boldsymbol{k}'\boldsymbol{l}})]^{1/2}} \quad (54)$$

As above, we take the polar axis parallel to $\boldsymbol{k}$ and measure azimuthal angles ϕ in the plane perpendicular to the plane defined by $\boldsymbol{k}$ and $\boldsymbol{k}'$ so that $\phi_{\boldsymbol{k}'} = 0$ and (40) holds.

The sum rules are slightly modified from those of OP-NOFT-Cs:

$$\sum_{\boldsymbol{k}} p_1(k) = N \,, \quad (55)$$

$$\sum_{\boldsymbol{k}'\neq\boldsymbol{k}} p_{11}(kk'\mu_{\boldsymbol{k}\boldsymbol{k}'}) = (N-1) p_1(k) \,. \quad (56)$$

The bounds are unchanged from those of OP-NOFT-Cs, Eqs. (44)-(46).

Converting the sums to integrals and scaling the wave vectors by k_F results in the energy functional

$$\mathcal{E}[p_1,p_{11}]=\frac{3}{4}{k_F}^2\int_0^\infty d\bar{k}p_1(\bar{k})\bar{k}^4$$
$$-\frac{9\pi n}{4{k_F}^2}\iint_0^\infty d\bar{k}d\bar{k}'\int_{-1}^1 d\mu_{\overline{\boldsymbol{k}\boldsymbol{k}'}}p_{11}(\bar{k}\bar{k}'\mu_{\overline{\boldsymbol{k}\boldsymbol{k}'}})\frac{\bar{k}^2{\bar{k}'}^2}{\bar{k}^2+{\bar{k}'}^2-2\bar{k}\bar{k}'\mu_{\overline{\boldsymbol{k}\boldsymbol{k}'}}}$$
$$+\frac{9\pi n}{2{k_F}^2}\iint_0^\infty d\bar{k}d\bar{k}'\int_{-1}^1 d\mu_{\overline{\boldsymbol{k}\boldsymbol{k}'}}\,S(\bar{k})S(\bar{k}')p_{10}^{1/2}(\bar{k}\bar{k}'\mu_{\overline{\boldsymbol{k}\boldsymbol{k}'}})p_{01}^{1/2}(\bar{k}\bar{k}'\mu_{\overline{\boldsymbol{k}\boldsymbol{k}'}})\xi(\bar{k}\bar{k}'\mu_{\overline{\boldsymbol{k}\boldsymbol{k}'}})$$
$$\times\frac{\bar{k}^2{\bar{k}'}^2}{\left(\bar{k}^2+{\bar{k}'}^2\right)^2-4\bar{k}^2{\bar{k}'}^2{\mu_{\overline{\boldsymbol{k}\boldsymbol{k}'}}}^2},\quad(57)$$

$$\xi(\bar{k}\bar{k}'\mu_{\overline{\boldsymbol{k}\boldsymbol{k}'}})=\frac{3\int_0^\infty d\bar{l}\,\bar{l}^2\int_{-1}^1 d\mu_{\overline{\boldsymbol{k}\boldsymbol{l}}}\int_0^{2\pi}d\varphi_{\bar{l}}\,p_{11}^{1/2}(\bar{k}\bar{l}\mu_{\overline{\boldsymbol{k}\boldsymbol{l}}})p_{11}^{1/2}(\bar{k}'\bar{l}\mu_{\overline{\boldsymbol{k}'\boldsymbol{l}}})}{4p_1(\bar{k})^{1/2}p_1(\bar{k}')^{1/2}}.\quad(58)$$

The sum rules become

$$\int_0^\infty d\,\bar{k}p_1(\bar{k})\bar{k}^2=2/3,\quad(59)$$

$$\int_0^\infty d\,\bar{k}'\int_{-1}^1 d\,\mu_{\overline{\boldsymbol{k}\boldsymbol{k}'}}p_{11}(\bar{k}\bar{k}'\mu_{\overline{\boldsymbol{k}\boldsymbol{k}'}})\bar{k}'^2=\frac{4}{3}p_1(\bar{k}),\quad(60)$$

completing the specification of the fully polarized OP-NSOFT-Ct.

5. Results

Computations were carried out by the method described in **I**. We represent $p_1(\bar{k})$ using a non-uniform radial k-mesh of 20 points which are more closely spaced in the vicinity of k_F. The OPs $p_{11}(\bar{k}\bar{k}'\mu_{\overline{\boldsymbol{k}\boldsymbol{k}'}})$ are represented using the same radial mesh for $\bar{k}$ and $\bar{k}'$ and an angular grid of 10 points for $\mu_{\overline{\boldsymbol{k}\boldsymbol{k}'}}$. Similarly, the integrations in $\xi(\bar{k}\bar{k}'\mu_{\overline{\boldsymbol{k}\boldsymbol{k}'}})$ we carried out over the same radial mesh for $\bar{k}$, $\bar{k}'$, and $\bar{l}$; the same angular mesh for $\mu_{\overline{\boldsymbol{k}\boldsymbol{k}'}}$, $\mu_{\overline{\boldsymbol{k}\boldsymbol{l}}}$, and $\mu_{\overline{\boldsymbol{k}'\boldsymbol{l}}}$; and same angular mesh of 10 points for $\varphi_{\bar{l}}$. All integrations involving p_1 or p_{11} are carried out using a numerical quadrature scheme where the kernels k^2, $1/k^2$, etc., are integrated analytically in each volume element. In this way precise integrals are obtained in spite of the rather coarse representation of p_1 and p_{11}.

The total energy per particle of the unpolarized (paramagnetic, PM) HEL, obtained from OP-NSOFT-Cs, and of the total energy per particle of the fully polarized (ferromagnetic, FM) HEL, obtained from OP-NSOFT-Ct, are reported in Fig. 1 for $r_s\leq 10$. We also report in the same figure the results of diffusion Monte Carlo (DMC) simulations for the same systems.[xvi] The DMC energies are very accurate and should be taken as a benchmark of our calculations. It is apparent from the figure that the OP-NSOFT-C curves lie above the corresponding DMC curves even though the ξ-approximation is not variational in the strict sense. They reproduce the

variation of the energy with r_s in a qualitatively correct way, indicating that the error of OP-NSOFT-C in each of the two systems is weakly dependent on r_s. In particular, the PM curve has a minimum at $r_s \cong 4$ while the FM curve has a minimum at $r_s \cong 5$, similar to the corresponding DMC results. However, the error of the OP-NSOFT-C energies, as measured by the distance from the corresponding DMC energies, is larger for the PM HEL than for the FM HEL, reflecting the more important relative role of electron correlations in the former. As a consequence, the transition from PM to FM HEL occurs at $r_s \cong 7.5$, an improvement over HF theory, which gives the transition at $r_s \cong 5.5$[xxvi] but still very far from the DMC result, which places the transition at $r_s \cong 75$.[xxvii] The DMC estimate corrects an earlier variational Monte Carlo estimate that placed the transition at $r_s \cong 26$.[xxviii] The difficulty in locating accurately the transition reflects the very small energy difference between the unpolarized and the fully polarized HEL at small densities ($r_s > 20$).[xxvii]

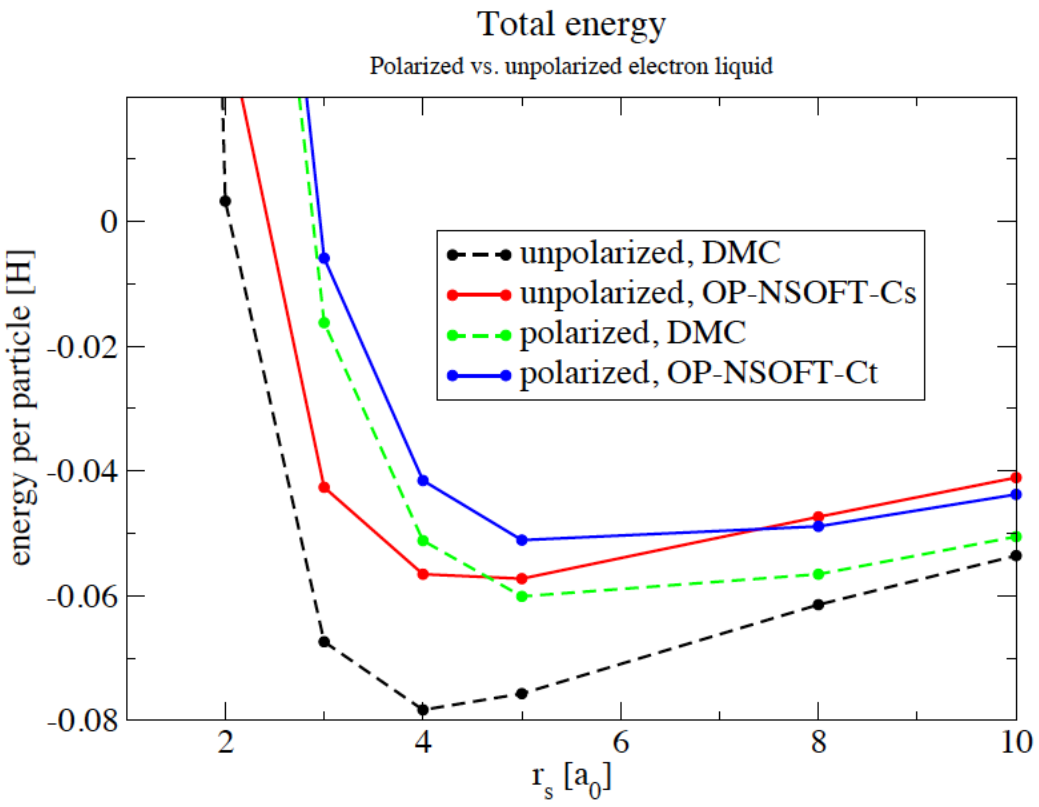

Figure 1. Total energy per particle vs r_s, $r_s = (1,10)$ for the unpolarized OP-NSOFT-Cs and polarized OP-NSOFT-Ct compared with the unpolarized and polarized DMC values of ref. xvi.

The correlation energy, i.e. the difference between the total energy and the HF energy, is reported in Fig. 2 in the r_s interval shown in Fig. 1. Comparing with the DMC data we see that

OP-NSOFT-Cs yields approximately one third of the PM DMC value throughout, while OP-NSOFT-Ct yields approximately from one half to one third of the FM DMC value with increasing r_s. As expected, the polarized correlation energy is significantly smaller because the correlation energy functional, which drives the correlation energy, has a smaller scattering matrix element and phase space and the exchange energy is larger in OP-NSOFT-Ct than in OP-NSOFT-Cs.

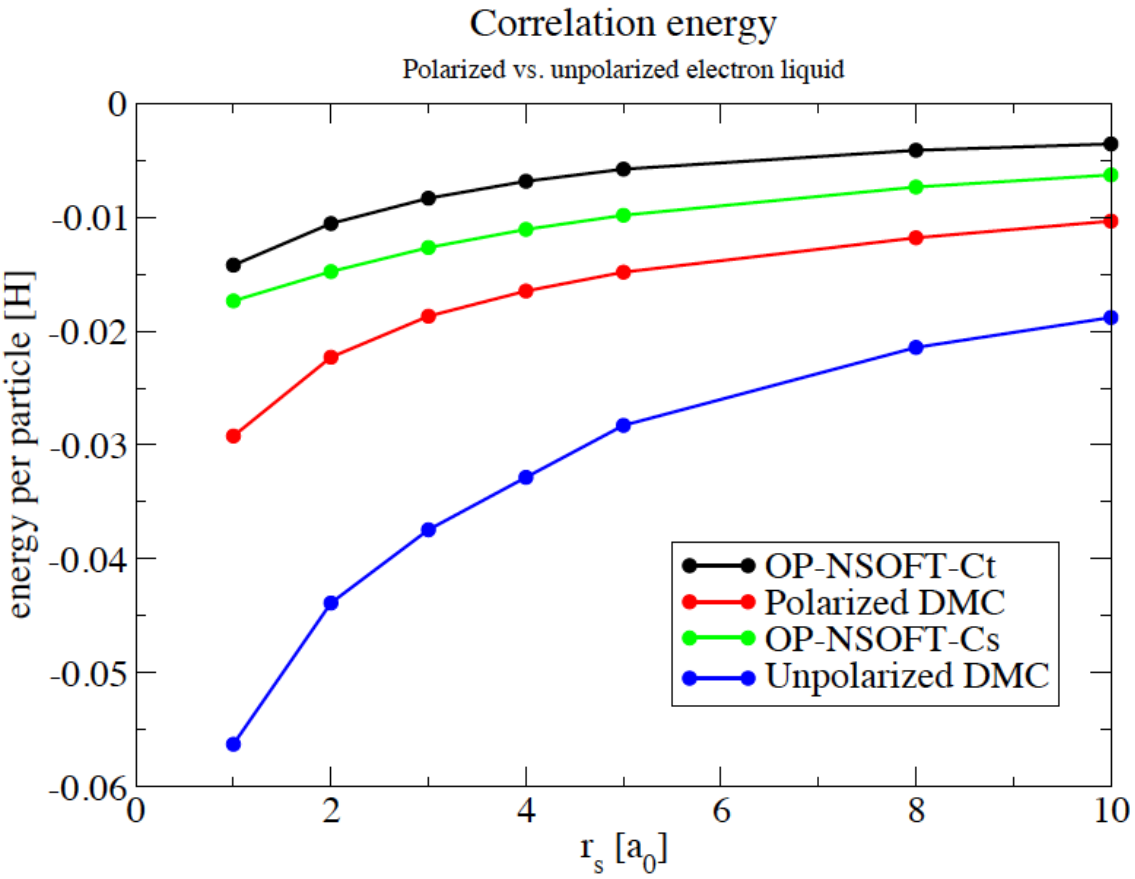

Figure 2. Correlation energy per particle vs r_s, $r_s = (1,10)$ for the unpolarized OP-NSOFT-Cs and polarized OP-NSOFT-Ct compared with the unpolarized and polarized DMC values of ref. xvi.

The various contributions to the OP-NSOFT-Cs,t energy functionals are displayed in Fig. 3 and Fig. 4. The PM HEL is illustrated in Fig. 3 in the interval $1 \leq r_s \leq 50$. The off-diagonal energy contribution is the correlation energy functional of the OP-NSOFT-Cs formalism: it should not be confused with the correlation energy defined as the difference of the total OP-NSOFT-Cs energy and its HF counterpart. At large r_s the exchange energy within OP-NSOFT-Cs converges to the HF energy, implying that, at these r_s values, the correlation energy is the sum of the off-diagonal and kinetic contributions. At large r_s the kinetic contribution decays to zero and the off-diagonal contribution converges to the correlation energy. The FM HEL is illustrated

in Fig.4 in the interval $1 \leq r_s \leq 10$. The off-diagonal contribution of the OP-NSOFT-Ct formalism is small. It and the correlation energy are nearly equal, implying that the correlation energy functional is too small to drive much change in the kinetic and exchange energies from their HF values.

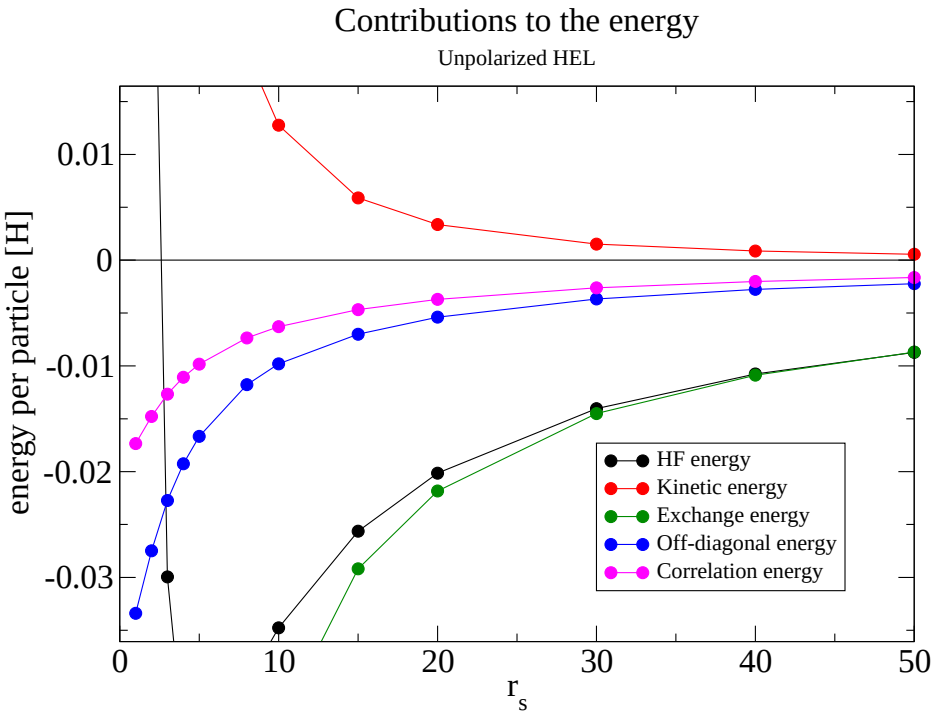

Figure 3. Contributions to the total energy per particle vs r_s, $r_s = (1,50)$ for OP-NSOFT-Cs. The off-diagonal energy is the value of E_C, the correlation energy functional, whereas the correlation energy is the difference between the total energy and the Hartree-Fock energy, which includes changes to the kinetic and exchange energies as well.

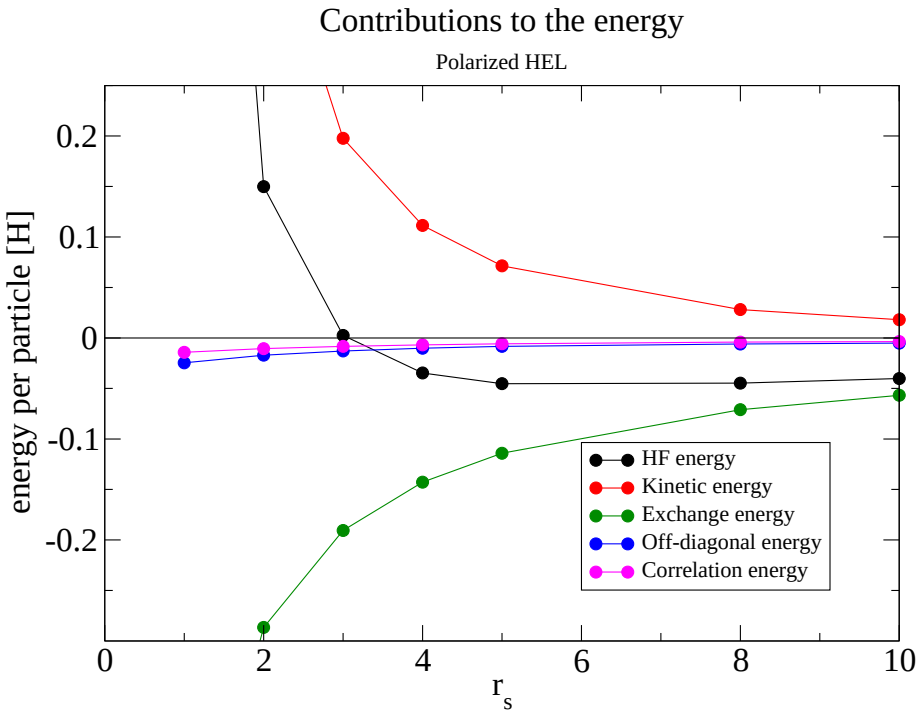

Figure 4. Contributions to the total energy per particle vs r_s, $r_s = (1,10)$ for OP-NSOFT-Ct.

To gain insight into electron correlation it is useful to analyze how the OPs change with r_s. The occupation probability $p_1(k)$ is shown in Fig.5 for the PM HEL for two density values, $r_s = 1$ and $r_s = 10$, respectively. DMC data[xvi] for this quantity are available and are reported in the same figure. We notice that all the data display a discontinuous jump at the Fermi wavenumber k_F in accordance with the Luttinger theorem. In Fig.5 the agreement of OP-NSOFT-Cs and DMC is quantitative for $r_s = 1$, where substantial correlation energy is obtained with little distortion of the free-particle or HF occupation probability. The agreement is only qualitative for $r_s = 10$, but reflects the trend of a reduced discontinuity with increasing r_s, cf Figure 10 below. The occupation probability $p_1(k)$ of the FM HEL is shown in Fig.6 at the same two densities as Fig.5. Only the OP-NSOFT-Ct results are reported in this figure, as the corresponding DMC data are not available. The occupation probability $p_1(k)$ differs negligibly from its free-electron or HF value at $r_s = 1$ and relatively little at $r_s = 10$ because the off-diagonal energy (correlation energy functional E_C) is smaller for the FM HEL, as shown in Fig.4.

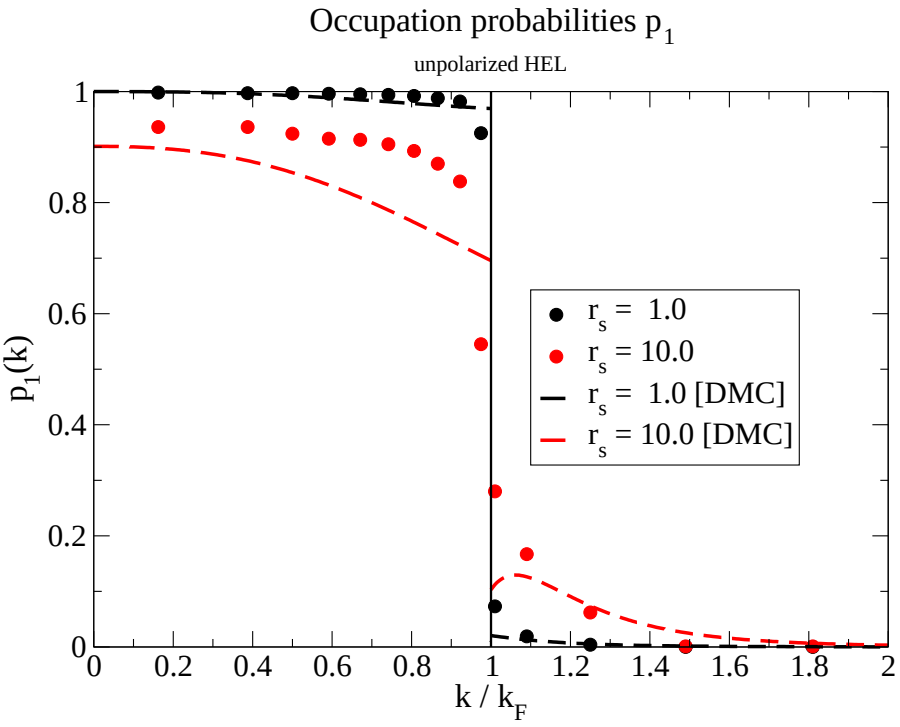

Figure 5. Occupation probability $p_1(k)$ vs k/k_F for OP-NOFT-Cs at $r_s = 1$ and 10 compared with the unpolarized DMC results. The dashed curves are the fitting functions that Ortiz and Ballone[xvi] fitted to their raw data. The maximum above k_F for $r_s = 10$ might be an artifact.

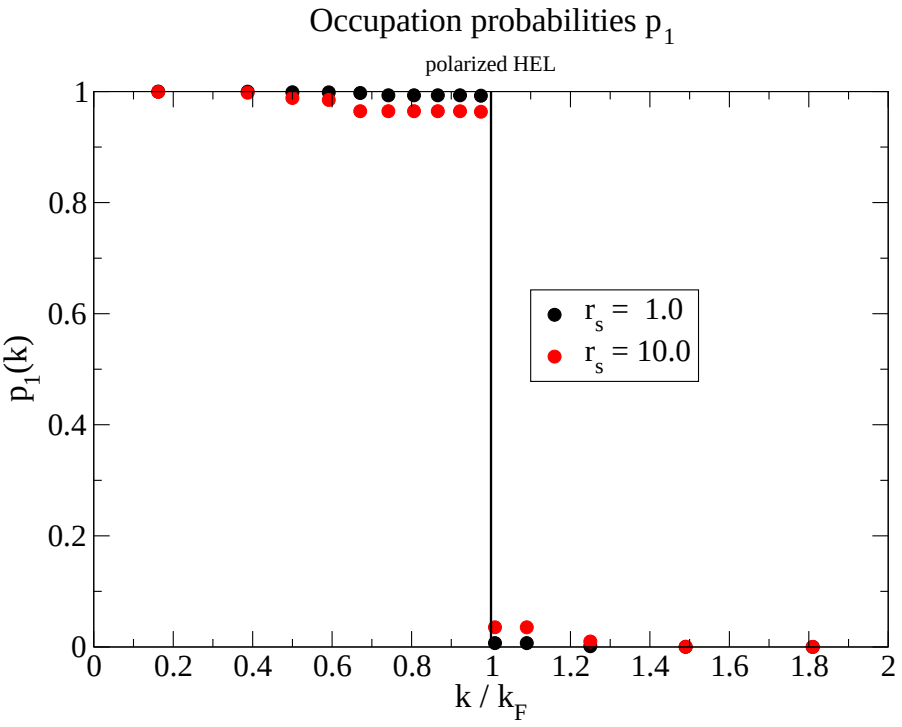

Figure 6. Occupation probability $p_1(k)$ vs k/k_F for OP-NSOFT-Ct at $r_s = 1$ and 10. There are no polarized DMC results available for comparison.

In the absence of correlation, $p_{11}(\boldsymbol{k},\boldsymbol{k}')$ factorizes into $p_1(k)p_1(k')$, which satisfies the sum rule (27) and bounds (29) and (30) for the PM and the corresponding conditions for the FM case. Inserting the factorized form into the expression (21) for $\xi(\boldsymbol{k}\boldsymbol{k}')$ yields unity for the PM case and the same for the equivalent of (21) in the PM case. Inserting this and the factorized form into the correlation energy functional E_C yields the positive definite form

$$E_C = \sum_{\boldsymbol{k}\neq\boldsymbol{k}'} \left\{S(k)\left[p_1(k)\left(1-p_1(k)\right)\right]^{½}\right\} w(|\boldsymbol{k}-\boldsymbol{k}'|) \left\{S(k')\left[p_1(k')\left(1-p_1(k')\right)\right]^{½}\right\}. \quad (60)$$

for the PM and similarly for the FM case. Minimizing the energy functional yields the HF state. Thus deviation from factorization of p_{11} is a sensitive measure of the extent of correlation. p_{11} enters into E_C via (20a,b). To reduce the contribution of a positive term to E_C, p_{11} should tend towards its upper bound. Conversely, to increase the magnitude of the contribution of a negative term, it should tend towards its lower bound. Thus deeper insight into electron correlation can be drawn from the angular dependence of the 2-OP $p_{11}(k,k',cos\theta)$ by its comparison there with its upper and lower bounds and the value of its factorized form. It is shown in Figs. 7, 8, and 9 for OP-NSOFT-Cs at $r_s = 10$. In Fig. 7, k equals k' and is greater than k_F. From (29), the lower bound of p_{11} is 0, and the upper bound is $p_1 = 0.167$ shown in red. At small angles p_{11} hugs its upper bound and undergoes a rapid transition towards its lower bound

starting at $\theta \cong 1.0$ rad. Because both k and k' are greater than k_F, the sign of the contribution to E_C is positive according to (9), so that according to (38) and (39a,b) the larger the value of p_{11}, the smaller the repulsive contribution to E_C and the larger the attractive contribution of the exchange energy to the total energy. This tendency is particularly important at smaller angles, the matrix element diverging at $\theta = 0$. However, if p_{11} were maximal at all θ, the sum rule (43) would be violated, so a compensating transition towards the minimal value occurs at larger θ, where the matrix element is weaker. This illustrates how the correlation hole that screens the tail of the Coulomb interaction is built up. The uncorrelated value of p_{11}, ${p_1}^2$, much less than the upper bound reached below the transition, is shown in blue to illustrate the magnitude of the correlation driven by the small angle scattering.

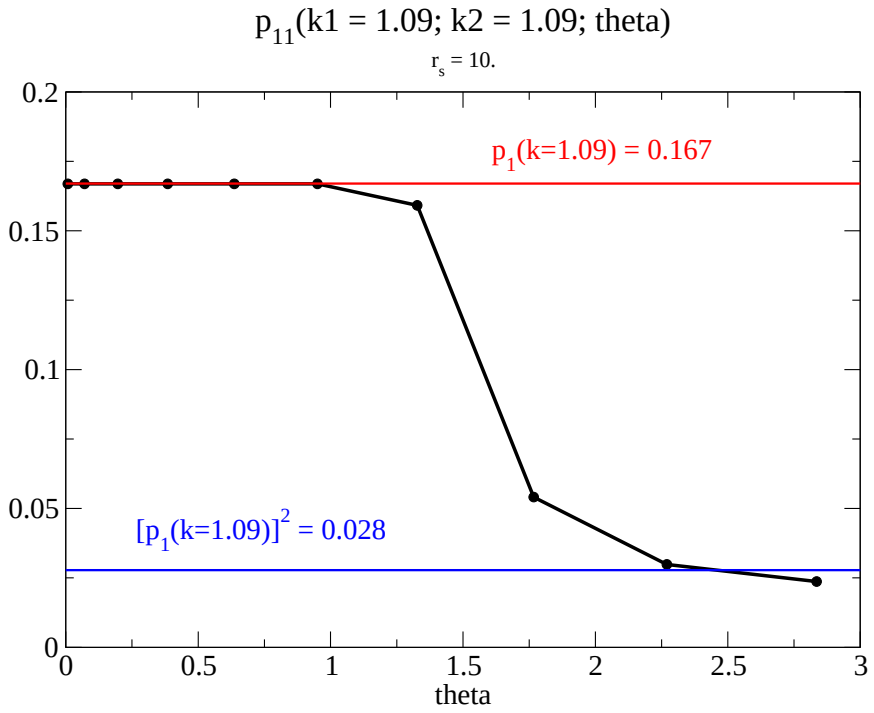

Figure 7. $p_{11}(k, k', cos\theta)$ vs θ for OP-NSOFT-Cs at $r_s = 10$, $k = k' = 1.09$, and $\theta = (0, 160°)$. The upper bound is shown in red, the uncorrelated value in blue, and the lower bound is 0.

In Fig. 8, k again equals k' but is less than than k_F. The behavior of p_{11} is similar to that in Fig. 7 for the same reasons. From (29), the lower bound of p_{11} is $2p_1 - 1 = 0.676$, and the upper bound is $p_1 = 0.838$, both shown in red. p_{11} hugs its upper bound to larger angles than in Fig. 7 and undergoes a more rapid transition starting at $\theta \cong 1.3$ rad and reaching its lower bound by $\cong 2.25$ rad. As in Fig. 7, the transition occurs because the sign of the contribution to the correlation energy functional is positive, k and k' both being smaller than k_F, while the

exchange energy is negative. The transition occurs at larger angles and is much sharper than in Fig. 7, because the value of p_1 is so much larger, as inspection of the correlation energy functional shows.

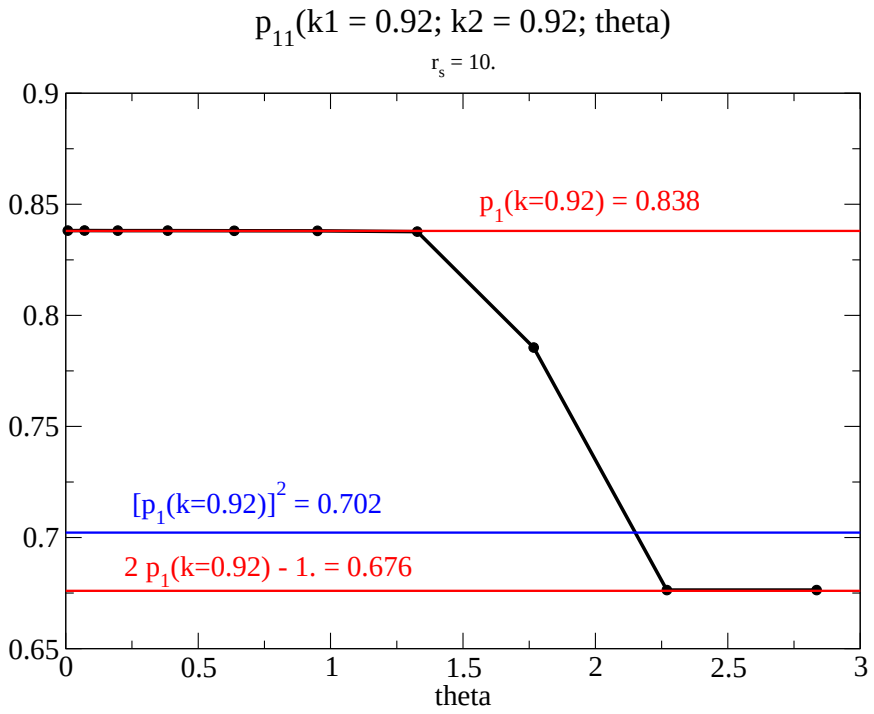

Figure 8. $p_{11}(k, k', cos\theta)$ vs θ for OP-NSOFT-Cs at $r_s = 10$, $k = k' = 0.92$, and $\theta = (0, 160°)$. The upper and lower bounds are shown in red and the uncorrelated value in blue.

Fig. 9 shows p_{11} with $k < k_F$ and $k' > k_F$ so that the sign of the contribution to the correlation energy functional is negative. Maximizing its magnitude requires *minimizing* p_{11}, the opposite of the cases in Figs. 7 and 8, whereas the magnitude of the exchange energy increases with p_{11}, a conflict. So, p_{11} hugs its lower bound $p_1(k) + p_1(k') - 1 = 0.005$ until $\theta \cong 0.4$ rad, a smaller angle, as shown in blue, but never reaches its upper bound $p_1(k') = 0.167$, which is off scale. Its maximum value $\cong 0.08$ remains well below the uncorrelated value, $p_1(k)p_1(k') = 0.140$, illustrating again how small-angle scattering drives correlation through the negative contributions to the correlation energy functional.

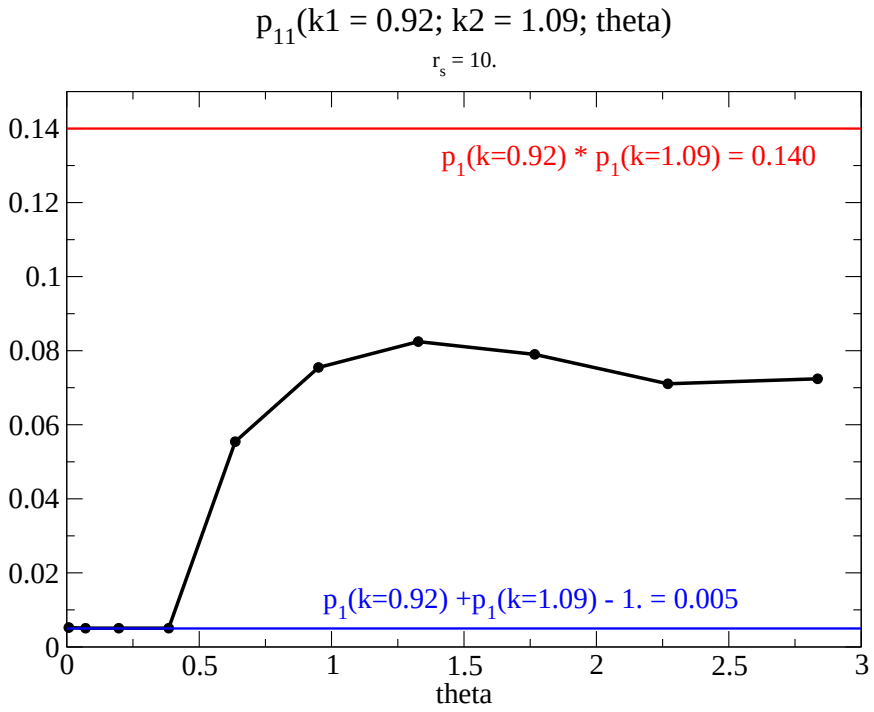

Figure 9. $p_{11}(k, k', cos\theta)$ vs θ for OP-NSOFT-Cs at $r_s = 10$, $k = 0.92$, $k' = 1.09$, and $\theta = (0, 160°)$. The lower bound is shown in blue, the uncorrelated value in red, and the upper bound is off scale.

Fig. 10 compares the r_s-dependence of the discontinuity Z in $p_1(k)$ at k_F obtained from OP-NSOFT-Cs with that obtained from DMC. Both curves trend downward smoothly with r_s, the OP-NSOFT-Cs curve more rapidly than the DMC curve, illustrating the over correlation of states near k_F in OP-NSOFT-Cs.

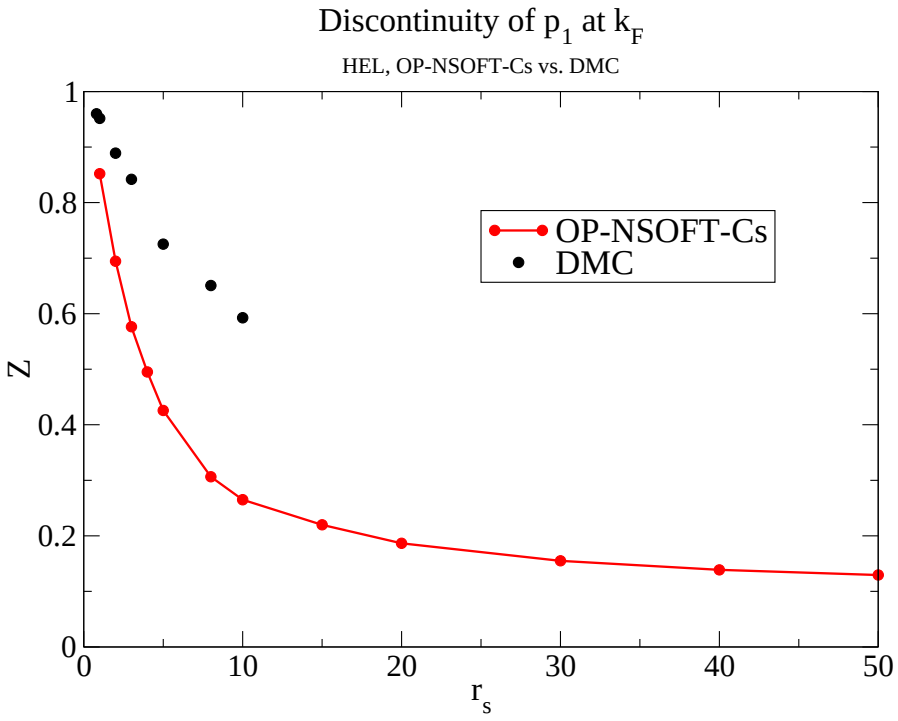

Figure 10. Discontinuity Z in $p_1(k)$ at k_F for OP-NSOFT-Cs, $r_s = (1{,}50)$ compared with DMC values, $r_s = (1{,}50)$.

6. A possible improvement

OP-NSOFT-Cs,t thus describes the 1-OP $p_1(k)$ acceptably and reveals interesting information about electron correlation through $p_{11}(\boldsymbol{k}, \boldsymbol{k}')$. The values of the correlation energy, ranging from ⅓ to ½ of the correct value, need significant improvement. There are four potential sources of that discrepancy: the PDC; the sign approximation; the pairing approximation; and the ξ-approximation. It is not possible to eliminate the PDC. That would require returning to the full orthogonality constraint of **I**, which is combinatorial. We presently see no way to improve the sign approximation. However, significant improvement could be expected from the full OP-NSOFT, which would include pairs of non-zero total momentum, increasing the phase space contributing to the correlation energy functional. Improvement of the ξ-approximation would occur in the full OP-NSOFT for the same reason.

7. Acknowledgement

Support for this work was provided by the Department of Energy under Award number DE-FG02-05ER46201. The authors are grateful to an anonymous referee for many excellent comments, particularly with regard to relating this work to the relevant literature.

8. Authors' Contributions

RG's primary contribution was the computations. MHC's primary contribution was the formalism. RC's primary contribution was establishing goals and connecting the formalism and the computations. All contributed equally to the interpretation and evaluation of the results.

---

[i] Hohenberg P, and Kohn W 1964 Inhomogeneous electron gas *Phys. Rev.* **136** B864.

[ii] Kohn W, and Sham L J 1965 Self-consistent equations including exchange and correlation effects *Phys. Rev.* **140** A1133.

[iii] Gilbert T L 1975 Hohenberg-Kohn theorem for nonlocal external potentials *Phys. Rev. B* **12** 2111.

[iv] Piris M 2017 Global Method for Electron Correlation *Phys. Rev. Lett.* **119** 063002.

[v] van Meer R, Gritsenko O V, and Baerends E J 2018 A non-JKL density matrix functional for intergeminal correlation between closed-shell geminals from analysis of natural orbital configuration interaction expansions *J. Chem. Phys.* **148** 104102.

[vi] Pernal K, and Giesbertz K J H 2016 Reduced Density Matrix Functional Theory (RDMFT) and Linear Response Time-Dependent RDMFT (TD-RDMFT) *Top. Curr. Chem.* **368** 125.

[vii] Herbert J M, and Harriman J E 2003 Self-interaction in natural orbital functional theory *Chem. Phys. Lett*. **382** 142.

[viii] Piris M 2013 A Natural Orbital Functional Based on an Explicit Approach of the Two-Electron Cumulant *Int. J. Quantum Chem.* **113** 620.

[ix] Piris M, and Ugalde J M 2014 Perspective on Natural Orbital Functional Theory *Int. J. Quantum Chem.* **114** 1169

[x] Coleman A J 1963 Structure of fermion density matrices *Rev. Mod. Phys.* **35** 668; Garrod C, and Percus J K 1964 Reduction of the N-particle variational problem *J. Math. Phys.* **5** 1756; Percus J 2013 On the trail of the 2-body reduced density matrix *Comput. Theor. Chem.* **1003** 2.

[xi] Zhao Z, Braams B J, Fukuda M, Overton M L, and Percus J K 2004 The reduced density matrix method for electronic structure calculations and the role of the three-index representability conditions *J. Chem. Phys.* **120** 2095; Nakata M, Nakatusuji H, and Ehara M 2001 Variational claculations of fermion second-order reduced density matrices by semidefinite programming algorithm *J. Chem. Phys.* **114** 8282; Gidofalvi G, and Mazziotti D A 2008 Active-space two-electron reduced-density-matrix method: Complete active-space calculations without diagonalization of the N-electron Hamiltonian, *J. Chem. Phys.* **129** 134108.

[xii] Gebauer R, Cohen M H, and Car R 2016 A well-scaling natural orbital theory *Proc. Nat. Acad. Sci.* **113** 46*;* referred to as **I**. There, the acronym used was OP-NOFT for occupation-probability-based natural-orbital functional theory, which here has been replaced by OP-NSOFT occupation-probability-based natural-spin-orbital functional theory as more accurate.

[xiii] Löwdin P O 1955 Quantum Theory of Many-Particle Systems I. Physical Interpretations by Means of Density Matrices, Natural Spin-Orbitals, and Convergence Problems in the Method of Configurational Interaction *Phys. Rev.* **97** 1474.

[xiv] Mazziotti D A 2008 Parametrization of the Two-Electron Reduced Density Matrix for its Direct Calculation without the Many-Electron Wave Function *Phys. Rev. Lett.* **101** 253002.

[xv] Piris M, Matxain J M, and Lopez X 2013 The intrapair electron correlation in natural orbital functional theory *J. Chem. Phys.* **139** 234109.

[xvi] Ceperly D M, and Alder B J 1980 Ground state of the electron gas by a stochastic method *Phys. Rev. Lett.* **45** 566; Ortiz G and Ballone P 1994 Correlation energy, structure factor, radial distribution function, and momentum distribution of the spin-polarized uniform electron gas *Phys. Rev. B* **50** 1391; Ortiz G and Ballone P 1997 Erratum *Phys. Rev. B* **56** 9970.

[xvii] Lathiotakis N N, Helbig N, and Gross E K U 2007 Performance of one-body reduced density-matrix functionals for the homogeneous electron gas *Phys Rev B* **75** 195120.

[xviii] Bardeen J, Cooper L N, and Schrieffer J R 1957 Microscopic Theory of Superconductivity *Phys. Rev.* **106** 162.

[xix] Leggett A J 1972 Interpretation of Recent Results on He3 below 3 mK: A New Liquid Phase? *Phys. Rev. Lett.* **29** 1227.

[xx] Pernal K, and Cioslowski J 2004 Phase dilemma in density matrix functional theory *J. Chem. Phys.* **120** 5987.

[xxi] Ayers P W, and Liu S 2007 Necessary and sufficient conditions for the N-representability of density functionals *Phys. Rev. A* **75** 022514; Ayers P W, and Davidson E R 2007 Linear inequalities for diagonal elements of density matrices *Adv. Chem. Phys.* **134** 443.

[xxii] Lukman B, Koller J, Borstnik, and Azman A (1970) Calculations on molecular systems with the Hartree-Fock-Bogoliubov self-consistent-field method *Mol. Phys.* **18** 857; England W B 1982 Ordinary Field-Theoretic Methods for Self-Consistent Wave Functions Which Describe Bond Formation and Dissociation *J. Phys. Chem.* **86** 1204; England W B 1983 Ordinary Field-Theoretic Methods for Self-Consistent Wave Functions Which Describe Bond Formation and Dissociation. II. Commutative Coupling Case *Int. J. Quantum Chem.* **23** 905; Piris M, and Cruz R 1995 A BCS Approach to Molecular Correlation *Int. J. Quantum Chem.* **53** 353; Piris M, Montero LA, and Cruz N 1997 A Bardeen-Cooper-Schrieffer approach to electron correlation in the density matrix formalism *J. Chem. Phys.* **107** 180; Staroverov V N, and Scuseria G E 2002 Assessment of simple exchange-correlation energy functionals of the one-particle density matrix *J. Chem. Phys.* **117** 2489; Staroverov V N, and Scuseria G E 2002 Optimization of density matrix functionals by the Hartree-Fock-Bogoliubov method *J. Chem. Phys.* **117** 11107; Csanyi G, and Arias T A 2000 Tensor product expansions for correlation in quantum many-body systems *Phys. Rev. B* **61** 7348.

[xxiii] Piris M, and Otto P 2000 The improved Bardeen-Cooper-Schrieffer method in polymers *J. Chem. Phys.* **112** 8187.

[xxiv] Blatt J M 1960 Electron Pairs in the Theory of Superconductivity *Prog. Theor. Phys.* **23** 447; Coleman A J 1965 Structure of Fermion Density Matrices. II. Antisymmetrized Geminal Powers *J. Math. Phys.* **6** 1425; Bratoz S, and Durand Ph 1965 Transposition of the Theories Describing Superconducting Systems to Molecular Systems. Method of Biorbitals *J. Chem. Phys.* **43** 2670.

[xxv] Luttinger J M 1960 Fermi Surface and Some Simple Equilibrium Properties of a System of Interacting Fermions *Phys. Rev.* **119** 1153.

[xxvi] Bloch F 1929 Bemerkung zur Elektronentheorie des Ferromagnetismus und der elektrischen Leitfähigkeit *Z. Phys.* **57** 545.

[xxvii] Zong F H, Lin C, and Ceperley D M 2002 Spin polarization of the low-density three-dimensional electron gas *Phys. Rev. E* **66** 036703.

[xxviii] Ceperley D 1978 Ground state of the fermion one-component plasma: A Monte Carlo study in two and three dimensions *Phys. Rev. B* **18** 3126.